

# Structural Characterization of a Lanthanum Bistriflimide Complex, $\text{La}(\text{N}(\text{SO}_2\text{CF}_3)_2)_3(\text{H}_2\text{O})_3$ , and an Investigation of La, Sm, and Eu Electrochemistry in a Room-Temperature Ionic Liquid, $[\text{Me}_3\text{N}^n\text{Bu}][\text{N}(\text{SO}_2\text{CF}_3)_2]$

Anand I. Bhatt,<sup>†</sup> Iain May,<sup>\*†</sup> Vladimir A. Volkovich,<sup>†,§</sup> David Collison,<sup>‡</sup> Madeleine Helliwell,<sup>‡</sup> Ilya B. Polovov,<sup>§</sup> and Robert G. Lewin<sup>||</sup>

Centre for Radiochemistry Research, School of Chemistry, The University of Manchester, Oxford Road, Manchester, M13 9PL U.K., School of Chemistry, The University of Manchester, Oxford Road, Manchester, M13 9PL U.K., Rare Metals Department, Ural State Technical University, 19 Mira Street, Ekaterinburg 620002, Russia, and Nexia Solutions, BNFL, Sellafield, Seascale, Cumbria, CA20 1PG U.K.

Received December 21, 2004

The reduction of selected lanthanide cations to the zerovalent state in the room-temperature ionic liquid  $[\text{Me}_3\text{N}^n\text{Bu}][\text{TFSI}]$  is reported (where TFSI = bistriflimide,  $[\text{N}(\text{SO}_2\text{CF}_3)_2]^-$ ). The lanthanide cations were introduced to the melt as the TFSI hydrate complexes  $[\text{Ln}(\text{TFSI})_3(\text{H}_2\text{O})_3]$  (where Ln = La<sup>III</sup>, Sm<sup>III</sup> or Eu<sup>III</sup>). The lanthanum compound  $[\text{La}(\text{TFSI})_3(\text{H}_2\text{O})_3]$  has been crystallographically characterized, revealing the first structurally characterized f-element TFSI complex. The lanthanide in all three complexes was shown to be reducible to the metallic state in  $[\text{Me}_3\text{N}^n\text{Bu}][\text{TFSI}]$ . For both the Eu and Sm complexes, reduction to the metallic state was achieved via divalent species, and there was an additional observation of the electrodeposition of Eu metal.

## Introduction

Room-temperature ionic liquids (RTILs) are being investigated as novel solvent systems for a range of chemical processes that currently use volatile organic carbon-based solvents. RTILs generally possess good thermal stability with negligible vapor pressure and have been used as reaction media for organic synthesis, catalysis, and liquid–liquid extraction.<sup>1</sup> We are interested in the application of ionic liquids in the nuclear industry, where they have been previously studied for  $\{\text{UO}_2\}^{2+}$  complexation and  $\{\text{UO}_2\}^{2+}$ , Sr<sup>2+</sup>, and Cs<sup>+</sup> extraction.<sup>2</sup> There is also the potential for the displacement of high-temperature alkali and alkaline earth

halide melts by lower temperature salts in the electrochemical separation of U and Pu from irradiated nuclear fuel. Switching to LTILs (low-temperature ionic liquids) would decrease both the required operating temperature and the corrosive nature of the melt. Initial studies focused solely on chloroaluminate melts, but these melts are very hygroscopic and, thus, are unsuitable for bulk electrodeposition.<sup>3</sup>

In the past few years, less moisture-sensitive melts have been synthesized based on the bis((trifluoromethyl)sulfonyl)-

\* Author to whom correspondence should be addressed. E-mail: Iain.May@manchester.ac.uk.

<sup>†</sup> Centre for Radiochemistry Research, School of Chemistry, The University of Manchester.

<sup>‡</sup> School of Chemistry, The University of Manchester.

<sup>§</sup> Ural State Technical University.

<sup>||</sup> Nexia Solutions.

(1) See, for example: (a) Welton, T. *Chem. Rev.* **1999**, *99*, 2071. (b) Wassercheid, P.; Keim, W. *Angew. Chem., Int. Ed.* **2000**, *39*, 3772. (c) Blanchard, A.; Hancu, D.; Beckman, E. J.; Brenecke, J. F. *Nature* **1999**, *399*, 28. (d) Carlin, R. T.; Fuller, J. In *Molten Salts: From Fundamentals to Applications*; Guane-Escard, M., Ed.; Springer: New York, 2002, p 321.

(2) (a) Visser, A. E.; Jensen, M. P.; Laszak, I.; Nash, K. L.; Choppin, G. R.; Rogers, R. D. *Inorg. Chem.* **2003**, *42*, 2179. (b) Jensen, M. P.; Dzielawa, J. A.; Richert, P.; Dietz, M. L. *J. Am. Chem. Soc.* **2002**, *124*, 10665. (c) Dai, S.; Ju, Y. H.; Barnes, C. E. *Dalton Trans.* **1999**, 1201. (d) Dietz, M. L.; Dzielawa, J. A. *Chem. Commun.* **2001**, 2124. (e) Visser, A. E.; Swatloski, R. P.; Reichert, W. M.; Griffin, S. T.; Rogers, R. D. *Ind. Eng. Chem. Res.* **2000**, *39*, 3596. (f) Chaimont, A.; Engler, E.; Wipff, G. *Inorg. Chem.* **2003**, *42*, 5348. (g) Bradley, A. E.; Hatter, J. E.; Nieuwenhuyzen, M.; Pitner, W. R.; Seddon, K. R.; Thied, R. C. *Inorg. Chem.* **2002**, *41*, 1692. (h) Bradley, A. E.; Hardacre, C.; Nieuwenhuyzen, M.; Pitner, W. R.; Sanders, D.; Seddon, K. R.; Thied, R. C. *Inorg. Chem.* **2004**, *43*, 2503.

(3) (a) Hopkins, T. A.; Berg, J. M.; Costa, D. A.; Smith, W. H.; Dewey, H. J. *Inorg. Chem.* **2001**, *40*, 1820. (b) Smith, W. H.; Costa, D. A. *Los Alamos National Laboratory Report*, LA-UR 98-3669, **1999**. (c) Anderson, C. J.; Deakin, M. R.; Choppin, G. R.; D'olieslager, W.; Heerman, L.; Pruett, D. J. *Inorg. Chem.* **1991**, *30*, 4013.

amide (bistriflimide,  $[\text{N}(\text{SO}_2\text{CF}_3)_2]^-$ , TFSI) anion with either tertiary alkylammonium, pyrrolidinium, or methylmorpholinium cations.<sup>4</sup> These salts would appear to have large enough electrochemical windows to reduce electropositive actinide cations to the metallic state.<sup>5</sup> In addition, recent studies by Chen and Hussey have shown that  $\text{Cs}^+$  can be reduced and stripped at a mercury electrode from  $[\text{Bu}_3\text{MeN}][\text{TFSI}]$ .<sup>6</sup> We have reported the electrochemical properties of three Group 15-based salts of the general formula  $[\text{Me}_4\text{X}][\text{TFSI}]$ , where  $\text{X} = \text{N}, \text{P}, \text{and As}$ .<sup>7</sup> These salts have extremely large electrochemical windows both in the molten state and when used as supporting electrolytes in MeCN. The  $\text{Eu}^{2+/0}$  couple was observed in all three melts, and as the standard  $\text{Eu}^{2+/0}$  couple is more negative than either the  $\text{U}^{3+/0}$  or  $\text{Pu}^{3+/0}$  couple, these melts have real potential for use in U and Pu electrorefining.

If TFSI is to be used as the anion in a LTIL, then it has the potential to be the dominant ligand for any dissolved f-element cation. There are very few reported X-ray structures where TFSI behaves as a ligand, the first being the  $\text{Cu}^{\text{I}}$  complex  $[\text{Cu}(\text{CO})(\text{N}(\text{SO}_2\text{CF}_3)_2)]$ ,<sup>8</sup> where TFSI coordinates to the soft Cu center through the central N atom. There are also structural reports on the coordination of TFSI through N to  $\text{Fe}^{\text{II}}$  in  $[(\text{C}_5\text{H}_5)\text{Fe}(\text{CO})_2(\text{TFSI})]$  and through O to  $\text{Ti}^{\text{IV}}$  in  $[(\text{C}_5\text{H}_5)_2\text{Ti}(\text{TFSI})_2]$ ,<sup>9</sup> and there is a recent report on O coordination to Zn through both bridging and chelating TFSI in  $[\text{Zn}(\text{TFSI})_3]$ .<sup>10</sup>

In this paper, we report the first structurally characterized f-element TFSI complex,  $[\text{La}(\text{TFSI})_3(\text{H}_2\text{O})_3]$ , and the synthesis and spectroscopic characterization of the analogous  $\text{Sm}^{\text{III}}$  and  $\text{Eu}^{\text{III}}$  complexes. We have used these complexes to study lanthanide electrochemistry, and in particular reduction to the zerovalent state, in  $[\text{Me}_3\text{N}^n\text{Bu}][\text{N}(\text{SO}_2\text{CF}_3)_2]$ ,<sup>11</sup> a RTIL chosen for its cathodic stability and relative ease of synthesis.

## Experimental Section

**General.** All chemicals were reagent grade, obtained commercially, and used as supplied unless stated otherwise. Infrared spectra were obtained from a Bruker Equinox 55/Bruker FRA 106/5

- (4) (a) Matsumoto, H.; Kageyama, H.; Miyazaki, Y. *Chem. Commun.* **2002**, 1726. (b) Matsumoto, H.; Kageyama, H.; Miyazaki, Y. *Chem. Lett.* **2001**, 182. (c) Sun, J.; MacFarlane, D. R.; Forsyth, M. *Ionics* **1997**, *3*, 356. (d) MacFarlane, D. R.; Meakin, P.; Sun, J.; Amini, N.; Forsyth, M. *J. Phys. Chem. B* **1999**, *103*, 4164. (e) Sun, J.; Forsyth, M.; MacFarlane, D. R. *J. Phys. Chem. B* **1998**, *102*, 8858.
- (5) (a) Quinn, B. M.; Ding, Z.; Moulton, R.; Bard, A. J. *Langmuir* **2002**, *18*, 1734. (b) Murase, K.; Nitta, K.; Hirato, T.; Awakura, Y. *J. Appl. Electrochem.* **2001**, *31*, 1089. (c) Oldham, W. J., Jr.; Costa, D. A.; Smith, W. H. In *Ionic Liquids: Industrial Applications for Green Chemistry*, ACS Symposium Series; Rogers, R. D., Seddon, K. R., Eds.; American Chemical Society: Washington D. C., 2002; Vol. 818, p 188. (d) Kim, K.-S.; Choi, S.; Demberelnyamba, D.; Lee, H.; Oh, J.; Byoung-Bae, L.; Mun, S.-J. *Chem. Commun.* **2004**, 828.
- (6) Chen, P.-Y.; Hussey, C. L. *Electrochim. Acta* **2004**, *49*, 5125.
- (7) Bhatt, A. I.; May, I.; Volkovich, V. A.; Hetherington, M. E.; Lewin, B. *Dalton Trans.* **2002**, 4532.
- (8) Polyakov, O. G.; Ivanova, S. M.; Gaundinski, M. C.; Miller, S. M.; Anderson, O. P.; Strauss, S. H. *Organometallics* **1999**, *18*, 3769.
- (9) Oldham, W. J., Jr.; Williams, D. B. *Proc. Electrochem. Soc.* **2002**, 2002-19.
- (10) Earle, M. M.; Hakala, U.; Mcauley, B. J.; Nieuwenhuyzen, M.; Ramani, A.; Seddon, K. R. *Chem. Commun.* **2004**, 1368.
- (11) McFarlane, D. R.; Sun, J.; Golding, J.; Meakin, P.; Forsyth, M. *Electrochim. Acta* **2000**, *45*, 1271.

spectrometer with a coherent 500 mW laser as solid samples (10 mg) using an ATR Golden Gate attachment. Raman spectra were recorded on the same instrument in the solid state (20 mg samples). Both the IR and Raman spectra were recorded with a resolution of  $4\text{ cm}^{-1}$ . A Metrohm 836 Titrando was used for Karl Fischer titration measurements to determine the moisture content in  $[\text{Me}_3\text{N}^n\text{Bu}][\text{TFSI}]$ .

**Syntheses.** All three  $[\text{Ln}^{\text{III}}(\text{TFSI})_3(\text{H}_2\text{O})_3]$  complexes (where  $\text{Ln}^{\text{III}} = \text{La}^{\text{III}}, \text{Sm}^{\text{III}}$  or  $\text{Eu}^{\text{III}}$ ) were prepared by the reaction of  $\text{Ln}_2\text{O}_3$  and  $\text{HN}(\text{SO}_2\text{CF}_3)_2$  in  $\text{H}_2\text{O}$  in a 1:6 molar ratio. In a typical reaction, a solution of  $\text{HN}(\text{SO}_2\text{CF}_3)_2$  (8.75 g, 31.1 mmol) in  $\text{H}_2\text{O}$  (5 mL) was added to a suspension of  $\text{La}_2\text{O}_3$  (1.71 g, 5.2 mmol) in  $\text{H}_2\text{O}$  (5 mL), with stirring. After 10 min, the resultant clear solution was then placed in vacuo to remove  $\text{H}_2\text{O}$ , and any excess  $\text{HN}(\text{SO}_2\text{CF}_3)_2$ , yielding  $[\text{La}(\text{TFSI})_3(\text{H}_2\text{O})_3]$  as a microcrystalline solid. Yield: 9.14 g, 88.9%. Found: C, 6.95%; H, 0.70%; N, 4.16%; S, 18.26%; La, 12.68%. Calcd: C, 6.97%; H, 0.59%; N, 4.07%; S, 18.61%; La, 13.44%. For  $[\text{Sm}(\text{TFSI})_3(\text{H}_2\text{O})_3]$ , yield: 1.31 g, 97.7%. Found: C, 7.06%; H, 0.40%; N, 4.05%; S, 18.73%; Sm, 15.40%. Calcd: C, 6.90%; H, 0.58%; N, 4.02%; S, 18.41%; Sm, 14.39%. For  $[\text{Eu}(\text{TFSI})_3(\text{H}_2\text{O})_3]$ , yield: 4.78 g, 86.7%. Found: C, 7.17%; H, 0.72%; N, 3.99%; S, 17.34%; Eu, 15.04%. Calcd: C, 6.89%; H, 0.58%; N, 4.02%; S, 18.38%; Eu, 14.52%.

**Synthesis of *N,N,N*-Trimethyl-*n*-butylammonium Bis(trifluoromethanesulfonyl)amide,  $[\text{Me}_3\text{N}^n\text{Bu}][\text{TFSI}]$ .**  $\text{Me}_2\text{N}^n\text{Bu}$  (100 mL, 0.72 mol) was placed into a salt ice bath at  $-17\text{ }^\circ\text{C}$ . After 15 min, MeI (45 mL, 0.72 mol) was added dropwise over 1 h to form a white precipitate of  $[\text{Me}_3\text{N}^n\text{Bu}]\text{I}$ .  $\text{Et}_2\text{O}$  (100 mL) was then added to this precipitate with stirring.  $\text{H}_2\text{O}$  (100 mL) was added to the resultant suspension to dissolve the  $[\text{Me}_3\text{N}^n\text{Bu}]\text{I}$ , with the aqueous layer then separated and the  $\text{H}_2\text{O}$  removed in vacuo to form a white microcrystalline solid (yield of  $[\text{Me}_3\text{N}^n\text{Bu}]\text{I} = 127.79\text{ g}$ , 73.9%).  $\text{Li}[\text{TFSI}]$  (151.2 g, 0.53 mol) was dissolved in water (150 mL) and added to a solution of  $[\text{Me}_3\text{N}^n\text{Bu}]\text{I}$  (127.79 g, 0.53 mol) in water (200 mL) with stirring. The resultant pale-yellow-colored, water-immiscible liquid was extracted and washed with an aqueous solution of  $\text{Na}_2\text{S}_2\text{O}_3 \cdot 5\text{H}_2\text{O}$  (5 g, 10 mL). The liquid  $[\text{Me}_3\text{N}^n\text{Bu}][\text{TFSI}]$  was then dried in vacuo at  $110\text{--}130\text{ }^\circ\text{C}$  to yield a colorless clear liquid (yield = 181.63 g, 87.1%). Found: C, 27.21%; H, 4.78%; N, 6.98%; S, 16.18%. Calcd: C, 27.27%; H, 4.59%; N, 7.07%; S, 16.61%.

**Single-Crystal X-ray Diffraction.** Single-crystal X-ray diffraction experiments were undertaken on a Bruker platform CCD area detector diffractometer with the structure solved by direct methods followed by Fourier synthesis and then refined on  $F^2$ . The absolute configuration of  $[\text{La}(\text{TFSI})_3(\text{H}_2\text{O})_3]$  was determined by refining the Flack parameter. The important crystallographic data for  $[\text{La}(\text{TFSI})_3(\text{H}_2\text{O})_3]$  are given in Table 1 (see also the Supporting Information for CIF files).

**Electrochemical Measurements.** All of the voltammetric measurements were performed using an EG&G 273A potentiostat operated by model 250 Research Electrochemistry Software (M270), version 4.41. In all cases, a typical three-electrode cell was employed, comprising a large surface area Pt gauze counter electrode, a Ag wire quasi reference electrode or a  $\text{Ag}/\text{AgNO}_3$  ( $0.1\text{ mol L}^{-1}$  in MeCN) reference electrode, and a Pt disk working electrode ( $0.031\text{ cm}^2$ ). The working electrode was activated by freshly polishing the surface. Although the  $[\text{Me}_3\text{N}^n\text{Bu}][\text{TFSI}]$  ionic liquid exhibits hydrophobic characteristics and is stable under normal atmospheric conditions, cyclic voltammograms were recorded inside an inert atmosphere Ar drybox to minimize  $\text{O}_2$  and  $\text{H}_2\text{O}$  contamination. Prior to the measurements, solution resistance was measured using the  $iR$  compensation option in the model 250 Research

**Table 1.** Crystallographic Data for [La(TFSI)<sub>3</sub>(H<sub>2</sub>O)<sub>3</sub>]

empirical formula	C <sub>6</sub> H <sub>6</sub> F <sub>18</sub> LaN <sub>3</sub> O <sub>15</sub> S <sub>6</sub>
fw	1033.41
space group	<i>P</i> 2 <sub>1</sub> 3
cryst group	cubic
<i>a</i> (Å)	18.5702(15)
<i>b</i> (Å)	
<i>c</i> (Å)	
α (deg)	90
β (deg)	
γ (deg)	
<i>V</i> (Å <sup>3</sup> )	6404.0(9)
<i>Z</i>	8
<i>T</i> (K)	100
λ (Å)	0.71073
<i>D</i> <sub>calcd</sub> (mg M <sup>-3</sup> )	2.144
μ (mm <sup>-1</sup> )	0.1891
R1, wR2 indices ( <i>I</i> > 2σ <sup>2</sup> )	0.0394, 0.0865
R indices (all data)	0.0460, 0.0898

Electrochemistry Software, and all voltammograms were corrected by this value.

## Results and Discussion

**Synthesis, Spectroscopic and Structural Characterization of the Lanthanide Bistriflimide Complexes.** The [Ln<sup>III</sup>(TFSI)<sub>3</sub>(H<sub>2</sub>O)<sub>3</sub>] complexes (where Ln<sup>III</sup> = La, Sm, or Eu) were all characterized by chemical analysis and vibrational spectroscopy. The elemental analyses for all three complexes often indicated relatively poor agreement between found and calculated sulfur and lanthanide content. Repeated synthesis and analysis did not yield any better overall fit between found and calculated values, which can be attributed, at least in part, to the hygroscopic nature of the complexes.

Crystals of [La(TFSI)<sub>3</sub>(H<sub>2</sub>O)<sub>3</sub>] suitable for X-ray diffraction were grown from an aqueous solution under an Ar atmosphere over a period of several months. The crystal is cubic, space group *P*2<sub>1</sub>3. The asymmetric unit contains two crystallographically distinct {La(TFSI)(H<sub>2</sub>O)} units, which can be grown into two crystallographically distinct [La(TFSI)<sub>3</sub>(H<sub>2</sub>O)<sub>3</sub>] molecules by a 3-fold rotation axis passing through each of the two La centers. There are eight molecules in total in the unit cell. Both crystallographically distinct molecules contain three TFSI anions coordinated through an oxygen of each sulfonyl unit, forming three six-membered chelate rings bound to each La<sup>III</sup> cation. There are also three coordinated water molecules sitting adjacent to each other in a piano stool arrangement, yielding nine-coordinate La in both cases. The structures of both crystallographically distinct [La(TFSI)<sub>3</sub>(H<sub>2</sub>O)<sub>3</sub>] molecules are shown in Figure 1, with selected crystal data and bond lengths and angles given in Tables 1 and 2, respectively.

Each nine-coordinate La center has a distorted tricapped trigonal prismatic coordination geometry with respect to the coordinating oxygens. Looking along the 3-fold rotation axis, the coordinating waters sit on one triangular face of the prism (bottom) and the TFSI anions chelate through the top face and the capping positions. The TFSI anions bind to the La center in a propeller type arrangement. Four of the La centers in the unit cell have a Λ absolute configuration (designated La1 in Figure 1), and the remaining four have a Δ absolute configuration (designated La2).

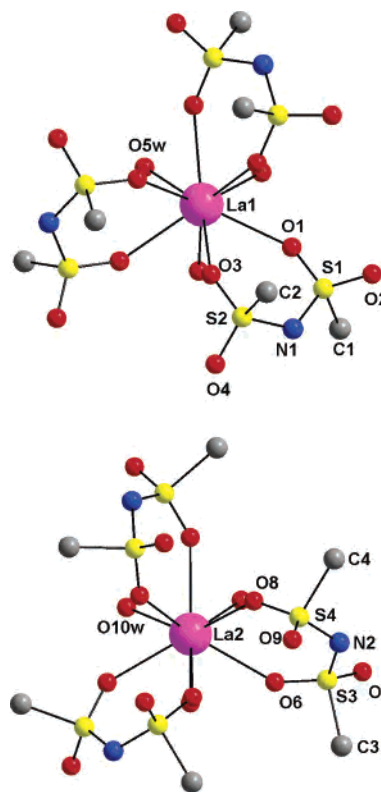


**Figure 1.** Structure of [La(TFSI)<sub>3</sub>(H<sub>2</sub>O)<sub>3</sub>] showing the Λ (La1) and Δ (La2) configurations. In both cases, the view is down the 3-fold rotation axis with coordinated waters on the bottom face of the tricapped trigonal prism and the TFSI<sup>-</sup> anion coordinated through the top face and the capping positions (H and F atoms omitted for clarity).

**Table 2.** Selected Bond Lengths (Å) and Angles (deg) for the Two Crystallographically Unique Molecules in [La(TFSI)<sub>3</sub>(H<sub>2</sub>O)<sub>3</sub>]

La1–O5 <sub>w</sub>	2.475(4)	La2–O10 <sub>w</sub>	2.489(4)
La1–O3	2.543(4)	La2–O8	2.539(4)
La1–O1	2.561(4)	La2–O6	2.547(4)
S1–O2	1.421(4)	S3–O7	1.413(7)
S1–O1	1.439(4)	S3–O6	1.421(5)
S1–N1	1.561(5)	S3–N2	1.544(8)
S1–C1	1.839(7)	S3–C3	1.860(12)
S2–O4	1.425(4)	S4–O9	1.395(6)
S2–O3	1.452(4)	S4–O8	1.444(4)
S2–N1	1.564(5)	S4–N2	1.573(7)
S2–C2	1.836(7)	S4–C4	1.818(10)
O2–S1–O1	116.8(3)	O7–S3–O6	116.6(3)
O2–S1–N1	113.1(3)	O7–S3–N2	108.3(5)
O1–S1–N1	114.5(3)	O6–S3–N2	115.0(3)
O2–S1–C1	104.9(3)	O7–S3–C3	103.2(5)
O1–S1–C1	104.3(3)	O6–S3–C3	103.6(5)
N1–S1–C1	100.9(3)	N2–S3–C3	109.3(6)
O4–S2–O3	116.6(2)	O9–S4–O8	117.1(3)
O4–S2–N1	110.5(3)	O9–S4–N2	116.8(5)
O3–S2–N1	115.1(3)	O8–S4–N2	112.4(3)
O4–S2–C2	105.9(3)	O9–S4–C4	104.9(3)
O3–S2–C2	103.6(3)	O8–S4–C4	104.9(4)
N1–S2–C2	103.6(3)	N2–S4–C4	97.5(5)
S1–N1–S2	125.3(3)	S1–N1–S2	126.0(3)
S1–O1–La1	146.8(2)	S3–O6–La2	144.1(3)
S2–O3–La1	146.3(2)	S4–O8–La2	139.9(3)

In the unit cell, the La complexes interact via intermolecular hydrogen bonding between the coordinated water molecules and the terminal oxygen atoms on the sulfonyl unit (O5<sub>w</sub> with O7/O9 and O10<sub>w</sub> with O2/O4), with OH<sup>+</sup>⋯O<sub>TFSI</sub> distances between 1.94 and 2.16 Å. Hydrogen bonding is only observed between Λ and Δ molecules, and

not between  $\Lambda/\Lambda$  or  $\Delta/\Delta$  [the shortest La–La distance between La(2) and La(1) is 8.07 Å].

In the  $\Delta$  configuration, the TFSI ligand forms a chelating ring in a distorted boat conformation (dihedral angle between C–S–S–C of 122.8°). In the  $\Lambda$  configuration, this boat conformation is further distorted with a C–S–S–C dihedral angle of 148.0°. The CF<sub>3</sub> orientations are different in the La complex from those in H[TFSI] (174.2°)<sup>12</sup> and in the K[TFSI] salt (17.12°).<sup>13</sup> In H[TFSI], the dihedral angle is consistent with CF<sub>3</sub> groups in a *transoid* orientation (with respect to the S–N–S plane); in the K salt, the dihedral angle is consistent with a *cisoid* orientation. Recently, *cisoid* and *transoid* orientations of the two CF<sub>3</sub> groups in TFSI have been observed in the structurally characterized 1,3-dimethylimidazolium and 1,2,3-triethylimidazolium TFSI salts, respectively.<sup>14</sup> The distorted *transoid* orientation of the CF<sub>3</sub> groups in both the  $\Lambda$  and  $\Delta$  molecules of [La(TFSI)<sub>3</sub>(H<sub>2</sub>O)<sub>3</sub>] is a result of the formation of a six-membered chelating ring.

Coordination of a La by an oxygen of the sulfonyl unit changes the achiral S center in the TFSI anion to a chiral center in the chelating ligand with both S centers in the TFSI ligand adopting an *R* configuration. This *R,R* configuration is observed for all TFSI ligands in each crystallographically distinct molecule. The *R,R* configuration of the TFSI anion is one of the possible orientations for the formation of a six-membered chelating ring (the other being an *S,S* configuration). It seems unlikely that an *R,S* mode would form a six-membered ring because of steric interferences (the *R,S* configuration would have groups *cisoid* with respect to the S–N–S plane).

[La(TFSI)<sub>3</sub>(H<sub>2</sub>O)<sub>3</sub>] is the first structurally characterized example of TFSI coordinated to an f-element and is also the first example of coordination through the sulfonyl oxygens to form a six-membered chelate ring. Coordination through the sulfonyl oxygens is in good agreement with a recent density functional theory study, which predicted bidentate sulfonyl coordination of [TFSI]<sup>−</sup> to M<sup>2+</sup> cations (M = Mg<sup>2+</sup>, Ca<sup>2+</sup>, Ba<sup>2+</sup>, Zn<sup>2+</sup> and Cu<sup>2+</sup>),<sup>15</sup> as recently experimentally observed for the Zn<sup>2+</sup> system.<sup>10</sup>

For coordinated water, the La–O bond length in each molecule (La1–O(5), 2.457(5) Å and La2–O(10) 2.489(4) Å) is significantly shorter than the corresponding La–O<sub>TFSI</sub> bond lengths (La1–O(3), 2.543(5) Å; La1–O(1), 2.561(4) Å; La2–O(8), 2.539(4) Å; and La2–O(6), 2.547(4) Å). They are also significantly shorter than the average La–water bond length in other nine-coordinate lanthanum complexes with coordinated water (2.605(14) Å),<sup>16</sup> and this is consistent with the poor ligating power/Lewis basicity of the TFSI anion.<sup>12</sup>

Turning to the TFSI anion, it can be seen that there is no appreciable lengthening of S–O, S–N, or S–C bonds on coordination or change in the S–N–S bond angle compared to the TFSI anion in the 1-ethyl-2-methyl-3-benzyl imidazolium salt.<sup>17</sup> Three of the four crystallographically distinct S–O–La bond angles are very similar (S1–O1–La1, 146.8(2)°; S2–O3–La1, 146.3(2)°; and S3–O6–La2, 144.1(3)°), with the fourth slightly smaller (S4–O8–La2, 139.9(3)°).

The TFSI anion is not expected to be a strongly coordinating ligand because the negative charge on the TFSI unit is not greatly delocalized into the S–O bond<sup>17</sup> and the CF<sub>3</sub> groups are strongly electron withdrawing. This certainly appears to be the case in [La(TFSI)<sub>3</sub>(H<sub>2</sub>O)<sub>3</sub>], with long La–O<sub>TFSI</sub> bond lengths in comparison with those of the coordinated water molecules and a lack of distortion in bond lengths, and angles, of the TFSI ligand on coordination.

The effect of coordination of TFSI to Ln<sup>III</sup> can also be probed by IR and Raman spectroscopy. Vibrational spectroscopic analysis of crystals of [La(TFSI)<sub>3</sub>(H<sub>2</sub>O)<sub>3</sub>] (both IR and Raman) indicate that the TFSI ligand is coordinated in an analogous manner in the crystalline sample used for X-ray diffraction and in the microcrystalline samples of [Ln(TFSI)<sub>3</sub>(H<sub>2</sub>O)<sub>3</sub>] (where Ln = La, Sm, or Eu) used for electrochemical measurements. The major IR and Raman bands of [TFSI]<sup>−</sup> have been fully assigned for both Li[TFSI] and H[TFSI],<sup>18</sup> and this work has been used as the basis for peak assignments for the three Ln<sup>III</sup> complexes. There are several distinct shifts in band position on coordination to Ln<sup>III</sup> cations. The Raman active  $\nu_s^{\text{sp}}$  SO<sub>2</sub> band shifts from 1131 cm<sup>−1</sup> in Li[TFSI] to 1148 cm<sup>−1</sup> in [La(TFSI)<sub>3</sub>(H<sub>2</sub>O)<sub>3</sub>], to 1147 cm<sup>−1</sup> in [Sm(TFSI)<sub>3</sub>(H<sub>2</sub>O)<sub>3</sub>], and to 1149 cm<sup>−1</sup> in [Eu(TFSI)<sub>3</sub>(H<sub>2</sub>O)<sub>3</sub>]. In Li[TFSI], the  $\nu_s^{\text{op}}$  SO<sub>2</sub> IR band is observed at 1138 cm<sup>−1</sup>. In the three lanthanide complexes, three bands are observed in this region, the major band occurring lower in energy, at 1105 cm<sup>−1</sup> in [La(TFSI)<sub>3</sub>(H<sub>2</sub>O)<sub>3</sub>], 1105 cm<sup>−1</sup> in [Sm(TFSI)<sub>3</sub>(H<sub>2</sub>O)<sub>3</sub>], and 1109 cm<sup>−1</sup> in [Eu(TFSI)<sub>3</sub>(H<sub>2</sub>O)<sub>3</sub>]. In addition, the  $\delta$  OH vibration for coordinated water can be clearly seen in the IR spectra of [La(TFSI)<sub>3</sub>(H<sub>2</sub>O)<sub>3</sub>] at 1632 cm<sup>−1</sup> and [Sm(TFSI)<sub>3</sub>(H<sub>2</sub>O)<sub>3</sub>] at 1630 cm<sup>−1</sup> but not in the less well-resolved IR spectrum of [Eu(TFSI)<sub>3</sub>(H<sub>2</sub>O)<sub>3</sub>]. The vibrational spectra with full peak assignments are provided in the Supporting Information.

**Electrochemistry.** The electrochemical window of pure [Me<sub>3</sub>N<sup>n</sup>Bu][TFSI] was measured at room temperature, referenced to Fc<sup>+</sup>/Fc,<sup>19</sup> and observed to be between −3.0 and 2.7 V (Figure 2). [Me<sub>3</sub>N<sup>n</sup>Bu][TFSI] would, therefore, appear to have an electrochemical window wide enough to support the reduction of U or Pu to the metallic state. As previously stated, our key industrial application is focused on the electrochemical separation of U and Pu from irradiated nuclear fuel, with an initial focus on the nonradioactive lanthanide elements. We have already shown that the Eu<sup>III/II</sup> and Eu<sup>II/0</sup> couples are observable in the high-temperature

(12) Haas, A.; Klare, Ch.; Betz, P.; Bruckman, J. Krüger, C.; Tsay, Y.-H.; Aübke, F. *Inorg. Chem.* **1996**, *35*, 1918.

(13) Zák, Z.; Růžička, A.; Michot, C. Z. *Kristallogr.* **1998**, *213*, 217.

(14) Holbrey, J. D.; Reichert, W. M.; Rogers, R. D. *Dalton Trans.* **2004**, 2267.

(15) Yong Li, X.; Nie, J. *J. Phys. Chem. A.* **2003**, *107*, 6007.

(16) (a) Aricó, E. M.; Zinner, L. B.; Kanellakopoulos, B.; Dornberger, E.; Rebizante, J.; Apostolodis, C. *J. Alloys Compd.* **2001**, *323–324*, 39. (b) Baggio, R.; Garland, M. T.; Perec, M.; Vega, D. *Inorg. Chem.* **1996**, *35*, 2396. (c) Wickleder, M. S. Z. *Anorg. Allg. Chem.* **1999**, *625*, 1794. (d) Benmerad, B.; Guebria-Laidoudi, A.; Balegroune, F.; Birkedal, H.; Chapuis, G. *Acta Crystallogr., Sect. C* **2000**, *C36*, 789. (e) Bataille, T.; Louër, D. *J. Mater. Chem.* **2002**, *12*, 3487.

(17) Golding, J. J.; MacFarlane, D. R.; Spiccia, L.; Forsyth, M.; Skelton, B. W.; White, A. H. *Chem. Commun.* **1998**, 1593.

(18) Rey, I.; Lindren, J.; Lassègues, J. C.; Grondin, J.; Servant, I. *J. Phys. Chem. A* **1998**, *102*, 3249.

(19) Gagné, R. R.; Koval, C. A.; Lisensky, G. C. *Inorg. Chem.* **1980**, *19*, 2854.

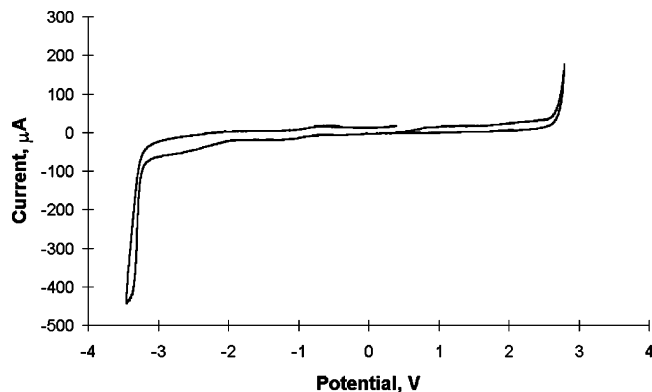


**Figure 2.** Cyclic voltammogram of pure  $[\text{Me}_3\text{N}^t\text{Bu}][\text{TFSI}]$  at room temperature.

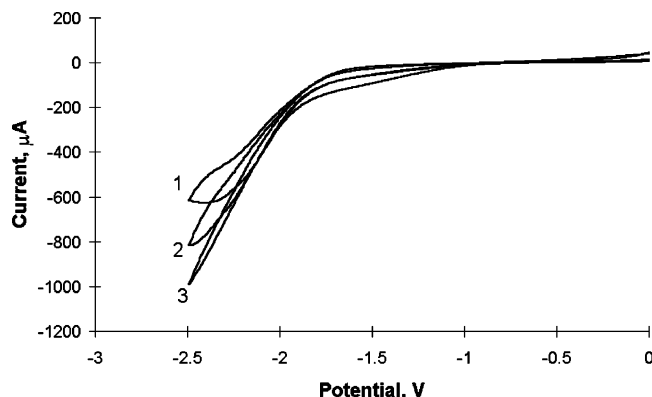


**Figure 3.** Cyclic voltammogram of  $[\text{La}(\text{TFSI})_3(\text{H}_2\text{O})_3]$  in  $[\text{Me}_3\text{N}^t\text{Bu}][\text{TFSI}]$ ,  $6.6 \times 10^{-2} \text{ mol L}^{-1}$  (1 =  $10 \text{ mV s}^{-1}$ , 2 =  $20 \text{ mV s}^{-1}$ , 3 =  $50 \text{ mV s}^{-1}$ ). Electrode surface area =  $0.0314 \text{ cm}^2$ .

melt,  $[\text{Me}_4\text{P}][\text{TFSI}]$ , at  $160 \text{ }^\circ\text{C}$ .<sup>7</sup> Because the standard  $E^\circ$  potential (vs the hydrogen electrode) of the  $\text{Eu}^{\text{II}/0}$  couple is  $-2.81 \text{ V}$  and for the  $\text{Pu}^{\text{III}/0}$  and  $\text{U}^{\text{III}/0}$  couples the potentials are  $-2.03$  and  $-1.80 \text{ V}$ , respectively, it would appear that U and Pu can, in principle, be reduced to the metallic state in this melt. However, plant operation would be greatly simplified by room-temperature operation, and thus, we have studied the electrochemistry of  $[\text{La}(\text{TFSI})_3(\text{H}_2\text{O})_3]$ ,  $[\text{Sm}(\text{TFSI})_3(\text{H}_2\text{O})_3]$ , and  $[\text{Eu}(\text{TFSI})_3(\text{H}_2\text{O})_3]$  in the RTIL  $[\text{Me}_3\text{N}^t\text{Bu}][\text{TFSI}]$ . It should be stated that this is a limited study, focusing on the basic electrochemical properties, and a more detailed investigation would be required to fully understand the electrochemistry of the three lanthanide systems.

It is well-known that lanthanum has only one stable oxidation state, +III (apart from zero), and that samarium and europium can additionally form ions in the oxidation state +II. Typical cyclic voltammograms of La-, Sm-, and Eu-containing systems are shown in Figures 3–5 (all potentials are given versus the  $\text{Fc}^+/\text{Fc}$  redox couple). Only one cathodic reduction peak was observed for La, with two observed for Sm and Eu. It is reasonable to assume that more positive peaks for Sm and Eu are associated with the corresponding III/II couples and more negative peaks for Sm and Eu, and the only one for La, are associated with the reduction to the metallic state. The approximate values of potentials of the cathodic peaks are  $-2.4 \text{ V}$  for  $\text{La}^{\text{III}}/\text{La}^0$ ,

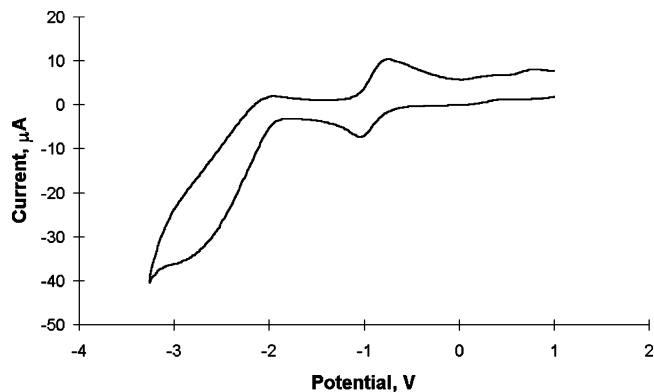


**Figure 4.** Cyclic voltammogram of  $[\text{Sm}(\text{TFSI})_3(\text{H}_2\text{O})_3]$  in  $[\text{Me}_3\text{N}^t\text{Bu}][\text{TFSI}]$ ,  $2.2 \times 10^{-1} \text{ mol L}^{-1}$ ,  $100 \text{ mV s}^{-1}$ . Electrode surface area =  $0.0314 \text{ cm}^2$ .

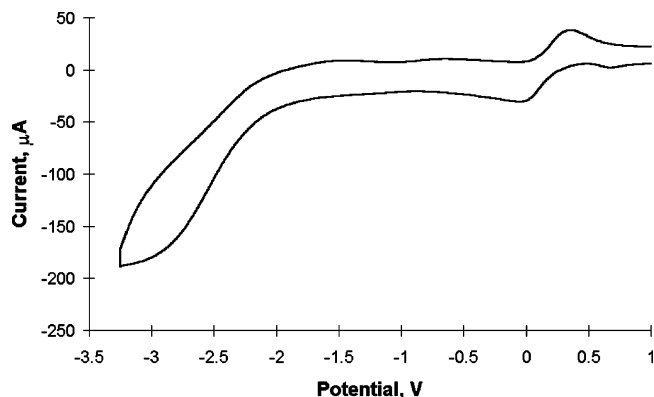


**Figure 5.** Cyclic voltammogram of  $[\text{Eu}(\text{TFSI})_3(\text{H}_2\text{O})_3]$  in  $[\text{Me}_3\text{N}^t\text{Bu}][\text{TFSI}]$ ,  $1.44 \times 10^{-1} \text{ mol L}^{-1}$ ,  $300 \text{ mV s}^{-1}$ . Electrode surface area =  $0.0314 \text{ cm}^2$ .

$-2.85 \text{ V}$  for  $\text{Sm}^{\text{II}}/\text{Sm}^0$ ,  $-3.0 \text{ V}$  for  $\text{Eu}^{\text{II}}/\text{Eu}^0$ ,  $-1.05 \text{ V}$  for  $\text{Sm}^{\text{III}}/\text{Sm}^{\text{II}}$ , and  $-0.05 \text{ V}$  for  $\text{Eu}^{\text{III}}/\text{Eu}^{\text{II}}$ . The difference between these potentials corresponds to the potentials of the above elements reported for aqueous solutions, high-temperature molten salts,<sup>20</sup> and ionic liquids.<sup>21</sup> There were, however, no anodic peaks that could be associated with the dissolution of reduced lanthanide metals.

Cyclic voltammograms measured for the Sm-containing melt centered around the  $\text{Sm}^{\text{III}}/\text{Sm}^{\text{II}}$  couple are shown in Figure 6. The observed peaks are reproducible at various scan rates, with anodic and cathodic peak separations increasing slightly with an increasing scan rate. If the reaction is diffusion-controlled (i.e. mass transfer), then the number of electrons transferred,  $n$ , can be calculated using either of the following two equations:

$$E_{\text{pa}} - E_{\text{pc}} = \frac{2.22RT}{nF}$$

$$E_{\text{pc}/2} - E_{\text{pc}} = \frac{2.20RT}{nF}$$

where  $E_{\text{pa}}$  and  $E_{\text{pc}}$  are the potentials of the anodic and cathodic peaks, respectively, and  $E_{\text{pc}/2}$  is the potential of the

(20) Nikolaeva, E. V.; Khokhlov, V. A. *Rasplavy* **2004**, *4*, 24.

(21) Yamagata, M.; Katayama, Y.; Miura, T. In *Molten Salts XIII, Proc. Int. Symp.*; The Electrochemical Society: Pennington, New Jersey, 2002; p 640.

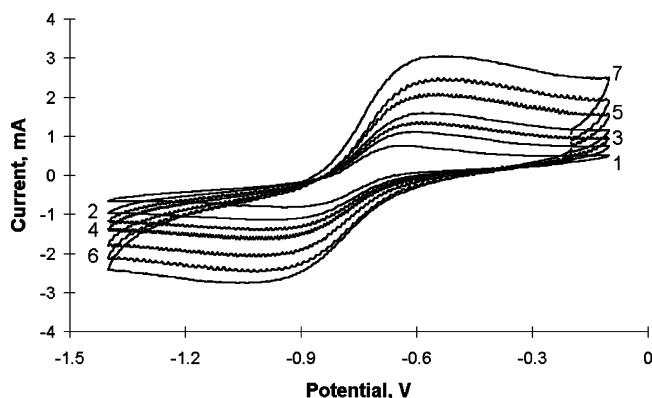


**Figure 6.** Cyclic voltammogram of  $\text{Sm}(\text{TFSI})_3(\text{H}_2\text{O})_3$  (0.041 mol/L) in  $[\text{Me}_3\text{N}^u\text{Bu}][\text{TFSI}]$ , focusing on the  $\text{Sm}^{\text{III/II}}$  couple at scan rates from 20 to 200  $\text{mV s}^{-1}$  (1–7, respectively). Electrode surface area = 0.196  $\text{cm}^2$ .

cathodic peak at half intensity. However, at low scan rates, the first equation gives a value of  $n = 0.1$ , whereas the second equation gives a value of  $n = 0.2$ , both unrealistic for what are presumed to be one-electron processes. The cathodic peak current is linearly dependent on the square root of the scan rate (see Supporting Information). This is indicative of either a purely diffusion or a purely kinetic mechanism of the reaction. Because, as shown above, the process is not mass-transfer-controlled (diffusion-controlled), then the reaction is controlled by the charge transfer (kinetics). The following equation can be used to calculate  $\alpha n$ , where  $\alpha$  = transfer coefficient:

$$E_{\text{pc}/2} - E_{\text{pc}} = \frac{1.857RT}{\alpha nF}$$

Calculated values of  $\alpha n$  were essentially independent of the scan rates, thus confirming that the reaction is controlled by the charge transfer. Using the obtained value of  $\alpha n = 0.21$  and the equation

$$i_p = 3 \times 10^5 n(\alpha n)^{1/2} A D_{\text{Ox}}^{1/2} V^{1/2} C_{\text{Ox}}$$

where  $C_{\text{Ox}}$  is the oxidant concentration (in this case,  $\text{Sm}^{\text{III}}$ ), it was possible to calculate the  $\text{Sm}^{\text{III}}$  diffusion coefficient,  $D_{\text{Ox}}$ . Assuming that  $n = 1$ ,  $D = 4.7 \times 10^{-8} \text{ cm}^2 \text{ sec}^{-1}$ . This value agrees well with that of  $3.2 \times 10^{-8} \text{ cm}^2 \text{ sec}^{-1}$  reported by Yamagata et al.<sup>21</sup> for  $\text{Sm}^{\text{III}}$  in somewhat more viscous 1-*n*-butyl-1-methylpyrrolidinium TFSI. The shape of the second reduction peak, and the absence of the corresponding anodic wave, is characteristic<sup>22</sup> for two consecutive, irreversible (charge-transfer-controlled) electrochemical reactions,  $\text{Sm}^{\text{III}} \rightarrow \text{Sm}^{\text{II}}$  and  $\text{Sm}^{\text{II}} \rightarrow \text{Sm}^0$ , Figure 4.

Similar behavior, especially at low scan rates, was observed in Eu-containing systems. A detailed analysis of cyclic and linear voltammograms also showed that  $\text{Eu}^{\text{III}}$  reduction also takes place in the kinetic regime. However, upon increasing scan rates, the cathodic peak gradually became less pronounced, Figure 7. It is likely that, at high scan rates, there is a change from two consecutive reactions ( $\text{Eu}^{\text{III}} \rightarrow \text{Eu}^{\text{II}}$  and  $\text{Eu}^{\text{II}} \rightarrow \text{Eu}^0$ ) to one three-electron reaction ( $\text{Eu}^{\text{III}} \rightarrow \text{Eu}^0$ ). Therefore, for  $\text{Eu}^{\text{III}}$ , it is only possible to obtain an approximate value for the diffusion coefficient for  $\text{Eu}^{\text{III}}$  of about  $10^{-7} \text{ cm}^2 \text{ sec}^{-1}$ .

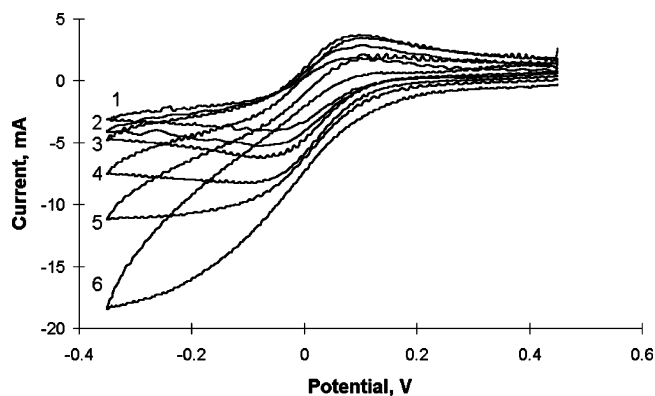


**Figure 7.** Cyclic voltammogram of  $\text{Eu}(\text{TFSI})_3(\text{H}_2\text{O})_3$  (0.052 mol/L) in  $[\text{Me}_3\text{N}^u\text{Bu}][\text{TFSI}]$ , focusing on the  $\text{Eu}^{\text{III/II}}$  couple at scan rates of 20, 40, 80, 120, 160, and 200  $\text{mV s}^{-1}$  (1–6, respectively). Electrode surface area = 0.196  $\text{cm}^2$ .

A separate series of experiments with a Eu-containing system was performed in the potentiostatic regime. The electrolysis was carried out at  $-3.1 \text{ V}$  overnight. A grey deposit was formed that, after washing off the excess ionic liquid with acetone, quickly oxidized in air to a white layered substance. This behavior is indicative of the formation of europium metal and its subsequent oxidation in air to  $\text{Eu}_2\text{O}_3$ , although there was an insufficient quantity of the sample for analysis.

Cyclic voltammograms of the La-containing system, Figure 3, have only one cathodic peak shifting toward negative values with increasing scan rates. This fact, as well as the absence of the corresponding anodic peak, suggests that the reaction  $\text{La}^{\text{III}} \rightarrow \text{La}^0$  is irreversible. Such irreversibility is probably due to slow charge-transfer kinetics. It may, though, be considered that metals formed on the cathode react with residual moisture associated both with the ionic liquid and with the introduced complexes after short reduction times. However, Karl Fischer titration results indicated  $<0.01\%$  water content, and the observation of Eu metal after operation in the potentiostatic regime indicates that moisture will not be a major issue. Similar irreversibility results were also observed in chloroaluminate melts by Tsuda and Ito.<sup>23</sup>

## Conclusion

In this study, we have reported the crystal and molecular structures of  $[\text{La}(\text{TFSI})_3(\text{H}_2\text{O})_3]$ , the first structurally characterized f-element TFSI complex and the first characterized TFSI complex bound to a metal cation through chelating sulfonyl oxygen atoms. The long  $\text{La}-\text{O}_{\text{TFSI}}$  bond lengths in comparison to the  $\text{La}-\text{O}_{\text{water}}$  bond lengths indicate that TFSI is a very weak ligand. Vibrational spectroscopy has been used to confirm that analogous complexes can be prepared with  $\text{Sm}^{\text{III}}$  and  $\text{Eu}^{\text{III}}$ . The electrochemical reduction of  $[\text{Ln}^{\text{III}}(\text{TFSI})_3(\text{H}_2\text{O})_3]$  species ( $\text{Ln} = \text{La}, \text{Sm}, \text{and Eu}$ ) down to  $\text{Ln}^0$  in the RTIL  $[\text{Me}_3\text{N}^u\text{Bu}][\text{TFSI}]$  indicates that it should be possible (from a comparison of  $E^\circ$  values) to reduce U and Pu to the metallic state in the same room-temperature melt,

(22) Polcyn, D. S.; Shain, I. *Anal. Chem.* **1966**, *38*, 370.

(23) Tsuda, T.; Ito, Y. *Proc. J. Electrochem. Soc.* **1996**, *143*, 914.

and these results indicate that this ionic liquid could be used for electrochemical separations in the nuclear industry.

**Acknowledgment.** We thank BNFL (Nexia Solutions) for funding (A.I.B. and V.A.V.), INTAS for a fellowship (I.B.P.) and C.A. Sharrad for Karl Fischer measurements.

**Supporting Information Available:** Crystallographic data in CIF format and additional vibrational spectroscopy and electrochemical data. This material is available free of charge via the Internet at <http://pubs.acs.org>.

IC048199U